Biomed Microdevices (2013) 15:1055–1066
DOI 10.1007/s10544-013-9797-1

Functionalized PLGA-doped zirconium oxide ceramics for bone tissue regeneration

Yael Lupu-Haber · Oded Pinkas · Stefanie Boehm · Thomas Scheper · Cornelia Kasper · Marcelle Machluf

Published online: 28 July 2013

Abstract Bone tissue engineering is an alternative approach to bone grafts. In our study we aim to develop a composite scaffold for bone regeneration made of doped zirconium oxide (ZrO_2) conjugated with poly(lactic-co-glycolic acid) (PLGA) particles for the delivery of growth factors. In this composite, the PLGA microspheres are designed to release a crucial growth factor for bone formation, bone morphogenetic protein-2 (BMP2). We found that by changing the polymer's molecular weight and composition, we could control microsphere loading, release and size. The BMP2 released from PLGA microspheres retained its biological activity and increased osteoblastic marker expression in human mesenchymal stem cells (hMSCs). Uncapped PLGA microspheres were conjugated to ZrO_2 scaffolds using carbodiimide chemistry, and the composite scaffold was shown to support hMSCs growth. We also demonstrated that human umbilical vein endothelial cells (HUVECs) can be co-cultured with hMSCs on the ZrO_2 scaffold for future vascularization of the scaffold. The ZrO_2 composite scaffold could serve as a bone substitute for bone grafting applications with the added ability of releasing different growth factors needed for bone regeneration.

Keywords PLGA · BMP2 · Scaffold · Drug delivery · Bone tissue engineering

Y. Lupu-Haber · O. Pinkas · M. Machluf
Faculty of Biotechnology and Food Engineering, Technion-Israel Institute of Technology, Haifa, Israel 32000

S. Boehm · T. Scheper · C. Kasper
Institute of Technical Chemistry, Leibniz University of Hannover, Callinstr. 5, 30167 Hannover, Germany

M. Machluf (✉)
The Laboratory of Cancer Drug Delivery & Cell Based Technologies, Faculty of Biotechnology & Food Engineering, Technion-Israel Institute of Technology, Haifa, Israel 32000
e-mail: machlufm@tx.technion.ac.il

1 Introduction

Bone is a dynamic tissue with the ability to heal and repair without scaring. Nevertheless, in cases of delayed union or large non-healing fractures resulting from trauma, tumors, infections or congenital abnormalities, bone graft procedures are required (Braddock et al. 2001). Current treatments for bone loss are autograft procedures, allograft procedures or bone graft substitutes such as metals and ceramics (Mourino and Boccaccini 2010; Porter et al. 2009). Such procedures are limited due to restricted availability and have high rates of complications such as donor site morbidity, pain, deep infections, hematomas, inflammations, and immune rejection (Khan et al. 2008; Salgado et al. 2004).

Bone tissue engineering, involving scaffolds, cells and growth factors, has emerged as an alternative approach to bone grafting that could overcome the above mentioned problems. Scaffolds for tissue engineering should be porous, three-dimensional, biocompatible and provide an environment that enables cells to proliferate and function. Moreover, bone graft substitutes should be osteoconductive, osteoinductive, easy to use and cost effective (Salgado et al. 2004). The use of different scaffold materials for bone tissue engineering has been reported: ceramics, polymers and their composites (Salgado et al. 2004). Composite scaffolds have the advantage of being osteoconductive, due to the ceramic component, while enabling a sustained release of growth factors from the polymeric component. Another key element in bone tissue engineering is the cell sources that are associated with bone formation as well as vascularization of the construct. Bone marrow derived mesenchymal stem cells (MSCs) are the main cell source utilized clinically and experimentally for bone tissue formation (Colnot 2011). MSCs are multipotent non-hematopoietic cells capable of self-renewal. Under appropriate conditions, MSCs have the capacity to differentiate into cells of different lineages including bone (Barry et al. 2001; Caplan 2007; Karp and Leng Teo 2009). MSCs are found

primarily in bone marrow but they have also been isolated from adipose tissues, peripheral blood and umbilical cord blood (Caplan 2007; Rosada et al. 2003). MSCs can easily be isolated from patients and cultured *in vitro*; they are also hypo immunogenic (Dominici et al. 2006). Other cells such as endothelial cells, also suggested as precursors for scaffold vascularization, which also affects bone tissue regeneration and may be a limiting factor for appropriate bone formation (Grellier et al. 2009; Lovett et al. 2009; Rouwkema et al. 2008). Often, to pre-vascularize bone tissue constructs, endothelial cells are co-cultured *in vitro* with bone cells or osteoprogenitor cells such as MSCs (Grellier et al. 2009; Kaully et al. 2009). Other studies initiated vascularization by adding growth factors that stimulate endothelial cell recruitment and proliferation (Chen et al. 2007; Richardson et al. 2001).

The last key element required for successful bone tissue engineering is growth factors. Growth factors expressed during fracture healing, have been studied and it is believed that the factors may serve as signaling agents that enhance bone formation in the tissue-engineered construct. One such important group are bone morphogenetic proteins (BMPs)—members of the transforming growth factor-β superfamily, with an important role in cell growth and bone formation (Lieberman et al. 2002; Reddi 1998). BMPs play a critical role in bone healing, as they are important regulators of MSC proliferation and osteogenic differentiation (Groeneveld and Burger 2000; Reddi 1998). Among the BMP family, BMP2 is one of the most potent osteoblastic differentiation inducers of mesenchymal progenitor cells and is clinically approved for the treatment of fractures and spinal fusions (Haidar et al. 2009; Xiao et al. 2007). BMP2, however, is a very expensive protein and a delivery system with local and sustained release will allow usage of lower amounts of BMP2.

PLGA-copolymers made of poly(lactic-co-glycolic acid), particles are extensively used for the delivery of proteins, drugs, and other factors such as cytokines and hormones (Benny et al. 2005; Joki et al. 2001; Kim et al. 2003; Mullerad et al. 2000). PLGA was approved by the FDA for drug delivery devices and is being studied extensively for use in other applications including cardiovascular diseases, cancer, vaccines and tissue engineering (Jain 2000; Lu et al. 2009). The advantages of PLGA particles are their technical versatility, biocompatibility and biodegradability (Berkland et al. 2003, 2002; Johansen et al. 1998). Various parameters such as polymer composition, size or surface properties can be customized to achieve different loadings and distinct polymer erosion profiles in order to control the release of encapsulated therapeutics (Vasir and Labhasetwar 2007; Walter et al. 2001, 1999).

In the current work we propose to improve zirconium oxide (ZrO_2) scaffolds for bone tissue engineering by conjugating PLGA microspheres that contain BMP2. The ability to engineer bone tissue is studied by culturing hMSCs, evaluating the biological activity of the released BMP2, and co-culturing hMSCs and HUVECs as a first step towards a vascularized bone construct.

2 Materials and methods

2.1 Preparation of PLGA microspheres

PLGA microspheres were prepared using the double-emulsion-solvent-extraction- technique. Briefly, 200 mg PLGA (Lactel®, Birmingham, AL) of various molecular weights (low MW-I.V:0.26–0.54 dL/g, medium MW-I.V: 0.55–0.75 dL/g, high MW-I.V: 0.95–1.20 dL/g) with a 50:50 lactic acid-to-glycolic acid ratio were dissolved in dichloromethane (BioLab®, Lawrenceville, GA). An aqueous solution (0.1 ml) containing protein, ribonuclease-I as a model protein or BMP2 (0.01–1 mg) in phosphate buffered saline was emulsified into the dissolved polymer using ULTRA-TURRAX® (IKA, Staufen, Germany) homogenizer at 12,000 rpm for 1 min on ice. The primary emulsion (W/O) was then emulsified into 1.5 ml of a 1 % (w/v) aqueous solution of polyvinyl alcohol (PVA) (Sigma-Aldrich™, St. Louis, MO) in DDW using homogenization at 6,000 rpm for 30 s on ice to form a multiple emulsion (W/O/W). The resulting emulsion was mixed with 50 ml of a 0.1 % (w/v) aqueous solution of PVA and stirred at room temperature for 5 min. Afterwards, 50 ml of a 0.1 % (w/v) PVA aqueous solution with 20 % iso-propyl-alcohol were added, and the solution was stirred for 30 min. The formed particles were recovered by centrifugation at 1,000 rpm and washed three times. Particles were re-suspended in water, lyophilized (Edwards™, Crawley, UK) and stored under desiccant condition at −20 °C.

2.2 PLGA particle morphology and size analysis

PLGA particle surface morphology and shape were studied using a Quanta 200 scanning electron microscope (FEI™, Hillsboro, OR). Average size and size distribution was determined by a laser diffraction particle size analyzer LS230 (Beckman Coulter Inc., Brea, CA).

2.3 Protein loading efficiency

Protein loading efficiency was determined by hydrolyzing 10–20 mg of loaded PLGA microspheres in 0.1 N NaOH. The total loading of ribonuclease-I and BMP2 in the microspheres was determined using the microBCA protein assay kit (Pierce™, Rockford, IL) and BMP2 Elisa detection kit (Peprotech Inc., Rocky Hill, NJ), respectively. The loading

efficiency was calculated as follows: the total protein loading amounts measured divided by the initial protein amount used for microsphere preparation.

2.4 Protein release kinetics from PLGA particles

The release of ribonuclease-I and BMP2 from PLGA microspheres was studied by incubating microspheres in PBS buffer (pH 7.4) at 37 °C with agitation for 4 weeks. At different time points, the upper medium was collected and replaced with fresh PBS and protein release was determined. Ribonuclease-I concentration was determined using the microBCA kit (Pierce™) and the BMP2 concentration was determined using BMP2 Elisa detection kit (Peprotech Inc.).

2.5 Cell culture

Human umbilical vein endothelial cells (HUVECs) were isolated from the lumen of the vessel wall using 1 mg/ml collagenase-I (Sigma-Aldrich™) for 30 min as previously described (Dahan et al. 2012). Human bone marrow derived MSCs (Lonza™, Basel, Switzerland) and HUVECs were cultured in alpha-MEM (Biological Industries™, Beit Haemek, Israel), supplemented with 5 ng/ml basic fibroblast growth factor (bFGF). Medium was supplemented with 10 % fetal bovine serum (Biological Industries™, Beit Haemek, Israel), 1 % Pen-Strep® (Invitrogen™, Carlsbad, CA), and 0.4 % Fungizone® (Invitrogen™). Osteoingenic differentiation was induced by cultivation in DMEM with D-glucose 1,000 mg/lit, L-glutamine, 0.05 mM ascorbic acid-2-phosphate, 10 mM β-glycerophosphate, and 0.1 μM dexamethasone (all purchased from Sigma-Aldrich™). Cultures were maintained at 37 °C in a humidified incubator with 5 % CO_2.

2.6 Biological activity of BMP2 released from PLGA microspheres

The biological activity of BMP2 released from the microspheres was evaluated using light microscopy and a real-time reverse-transcriptase polymerase chain reaction (real-time RT-PCR). For these studies, four experimental groups were investigated: I- hMSCs cultivated with microspheres loaded with 10 μg BMP2, II- and III- hMSCs cultivated without microspheres and hMSCs cultivated with empty microspheres made of capped PLGA (negative controls) and IV- hMSCs supplemented with 100 ng/ml free BMP2 (positive control). Changes in cell morphology and calcium deposition of differentiated hMSCs in comparison to undifferentiated hMSCs were followed for 12 days post cultivation using light microscopy (Eclipse TE 2000-S, Nikon, Tokyo, Japan) and the von Kossa staining method, respectively. When staining for von Kossa, cells seeded on cover slips were fixed with 4 % paraformaldehyde (PFA, Sigma-Aldrich™) for 30 min at room temperature, washed and incubated with 1 % silver nitrate (Carlo ERBA, Milan, Italy) for 20 min under UV light. Thereafter, samples were washed again, dehydrated through graded alcohol (70 %, 96 %, 100 %, each for 1 min), cleared in xylene and imaged using Eclipse TE 2000-S. Changes in the gene expression profiles of hMSCs were evaluated by real-time RT-PCR. After 14 days of culture, mRNA was isolated using Tri-Reagent (Sigma-Aldrich™) and 1 μg of total RNA was reverse transcribed using the VersoTM cDNA kit (Thermo Scientific Inc., Waltham, MA). Subsequently, cDNA was amplified using the Power SYBER® Green PCR Master Mix (Applied Biosystems™, Foster City, CA). The reaction was monitored using the 7300 Real-Time PCR System (Applied Biosystems™). Expression levels of the genes of interest (collagen-I, alkaline phosphatase, osteonectin, osteocalcin, bonesialoprotein) were normalized to the hGAPDH house keeping gene. Primers used for amplification of cDNA include:

- Collagen-I:

  forward: 5′-CTGGCCTCGGAGGAAACTTT-3′
  reverse: 5′-GGAAATTCCTCCGGTTGATTT-3′

- Alkaline phosphatase:

  forward: 5′-TTCCTGGGAGATGGGATGG-3′
  reverse: 5′-TTGTGGTGGAGCTGACCCTT-3′

- Osteonectin:

  forward: 5′-TGAGGACAACAACCTTCTGACTG-3′
  reverse: 5′-ATCTTCTTCACCCGCAGCTT-3′

- Osteocalcin:

  forward: 5′-CAAAGGTGCAGCCTTTGTGT-3′
  reverse: 5′-GCGCCTGGGTCTCTTCACTA-3′

- Bonesialoprotein:

  forward: 5′-GAGGAAGCAATCACCAAAATGA-3′
  reverse: 5′-TGAGAAAGCACAGGCCATTC-3′

- GAPDH:

  forward: 5′-CATGTTCGTCATGGGTGTGAA-3′
  reverse: 5′-GTGCAGGAGGCATTGCTGAT-3′

2.7 Cell cultivation on ZrO_2 scaffolds

hMSCs or HUVECs ($3\ 10^4$ cells/scaffold) were drop-wise seeded on pre-wetted ZrO_2 scaffolds (Sponceram®, Zellwerk, Eichstädt, Germany) in 24-well tissue culture plates and allowed to adhere for two hours. Scaffolds were then transferred to six-well tissue culture plates and growth medium was slowly added to each well. Cell viability on the

scaffolds was followed using AlamarBlue® cell viability assay (AbDserotec™, Oxford, UK) according to manufacturer's protocols. Three hours post incubation the fluorescence of 100 μl samples from each well was read using the Synergy HT Multi-Mode Microplate Reader (BioTek™, Winooski, VT) and fluorescence values were translated into cell number using a calibration curve.

2.8 Osteogenic differentiation of hMSCs on ZrO_2 scaffolds

ZrO_2 scaffolds seeded with hMSCs in standard growth medium or in osteoinductive growth medium were cultivated on ZrO_2 scaffolds for 60 days and then fixed with 4 % PFA (Sigma-Aldrich™) for 30 min at room temperature, stained with 0.01 mg/ml FITC-phalloidin (Sigma-Aldrich™) and 0.5 μg/ml DAPI (Sigma-Aldrich™) in PBS. Scaffolds were imaged with the LSM 700—Inverted confocal microscope (Zeiss, Oberkocahen, Germany). Mineralization was evaluated using the von Kossa staining protocol. Fixed scaffolds were incubated with 1 % silver nitrate for 20 min under UV light. Scaffolds were washed twice with DDW and incubated with 5 % thiosulfate for 5 min at room temperature. Scaffolds were then dehydrated through graded alcohol (70 %, 96 %, 100 %, each for 1 min) and cleared in xylene.

2.9 Co-culture of hMSCs and HUVECs on ZrO_2 scaffolds

For the co-culture experiments, hMSCs were seeded and cultured until cell number has reached 3 10^5 cells per scaffold, as determined by the AlamarBlue® assay (AbDserotec™). HUVECs expressing green fluorescent protein (GFP) were then seeded in a 1:1 ratio with hMSCs. After 30 days of co-culture on the ZrO_2 scaffolds, cells were fixed with 4 % PFA (Sigma-Aldrich™) for 30 min at room temperature, permeabilized with 0.1 % Triton-X-100 (Merck, Whitehouse Station, NJ) in PBS for 15 min at 4 °C and stained with 50 μg/ml propidium iodide (BD, Franklin Lakes, NJ). Scaffolds were imaged with the LSM 700 – Inverted confocal microscope (Zeiss, Oberkocahen, Germany).

2.10 Production of a composite scaffold

ZrO_2 scaffolds were pre-wetted in HEPES/NaOH buffer (pH 7) for one hour. Subsequently, the scaffolds were washed and 10 mg of microspheres made of uncapped PLGA (50:50) with a molecular weight of 0.55–0.75 dL/g were added to each scaffold with 1 mM Sulfo-EDC (Sigma-Aldrich™) and 30 μM NHS (Sigma-Aldrich™) in HEPES/NaOH buffer (pH 7). After 3 h, scaffolds were washed extensively in DDW for the removal of unattached microspheres. ZrO_2 scaffolds and composite scaffolds were imaged using a scanning electron microscope Quanta 200 (FEI™).

3 Results

3.1 Microsphere size and surface morphology

The shape and surface morphology of PLGA microspheres after freeze-drying was analyzed using scanning electron microscopy. PLGA particles had a spherical shape with a smooth surface area (Fig. 1a). The average size and size distribution of microspheres prepared from PLGA polymers differing in their molecular weights were determined using a laser diffraction instrument. All microsphere preparations had a narrow size distribution and the average particle diameter increased as the molecular weight of the polymer increased (Fig. 1b).

3.2 Microsphere loading and release profile

The effect of the polymer molecular weight and the initial protein loading on the loading efficiency was studied first on a model protein, ribonuclease-I, which resembles BMP2 in its molecular weight and isoelectric point. As seen in Fig. 2a, the loading efficiency increased when using polymers with higher molecular weights. However, increasing the initial loading of ribonuclease-I from 0.1 mg to 1 mg led to a decrease in the loading efficiency from 93 % to 54 %, respectively (Fig. 2b). All preparations were characterized by a burst release during the first days of the release. However, microspheres prepared with a low molecular weight polymer had a burst release of ~80 %, which was reduced to 50 % when using high molecular weight PLGA (Fig. 2c).

3.3 BMP2 loading and release kinetics

PLGA microspheres prepared from medium MW (0.55–0.75 dL/g) copolymers with ester end groups (capped) had a better BMP2 loading efficiency than PLGA microspheres composed of copolymers with acid end groups (uncapped, Fig. 3a). Microspheres prepared with capped PLGA microspheres had a smaller protein burst release (26 %) than uncapped PLGA microspheres (49 %, Fig. 3b). The effect of adding polyethylene glycol (PEG) to the internal phase was also tested, as it is known to limit penetration of protein to the interfacial film of the primary water-in-oil emulsion, which should result in a reduction of the burst release. However, the addition of PEG400 did not change the burst release of the protein (~50 %, Fig. 3b). All preparations exhibited a burst release after 1 day and complete release of BMP2 was achieved within 2 weeks of incubation.

3.4 Bioactivity of BMP2 released from PLGA microspheres

The biological activity of BMP2 released from microspheres composed of capped PLGA with a medium MW (0.55–

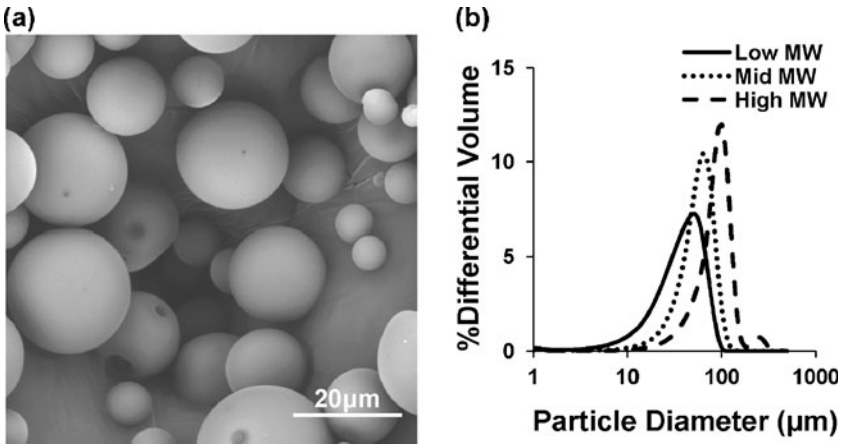

Fig. 1 Morphology and size of PLGA particles. Scanning electron microscopy image of PLGA particles (**a**). The effect of the PLGA molecular weight (low: 0.26–0.54 dL/g, mid: 0.55–0.75 dL/g, high: 0.95–1.20 dL/g) on the diameter distribution of the PLGA particles (**b**). Diameter was calculated as percent of particle volume in the sample

0.75 dL/g) was evaluated using light microscopy and von Kossa staining. For these studies, hMSCs were cultivated with PLGA microspheres for 12 days and the effect of the released BMP2 on cell morphology and calcium deposition was studied (Fig. 4). Undifferentiated hMSCs incubated without microspheres (negative control) proliferated in a well-organized pattern exhibiting elongated morphology and no calcium deposit. In contrast, hMSCs cultivated with free BMP2 (positive control) added to the growth medium grew in clusters and black dots indicative of calcium deposition were observed. hMSCs cultivated with empty microspheres had an elongated morphology, similar to the undifferentiated hMSCs, while hMSCs cultivated with microspheres loaded with BMP2 had also grown in clusters and showed light calcium deposition similar to the positive control. Real time RT-PCR analysis of hMSCs cultivated with BMP2-loaded microspheres for 2 weeks demonstrated increased expression levels of the collagen-I and osteonectin genes, which are indicative of osteogenic differentiation (Fig. 4c). Osteonectin was significantly increased compared to the positive control and empty microsphere groups. Alkaline phosphatase, bonesialoprotein and osteocalcin genes were not induced by free BMP2 or BMP2 released from PLGA microspheres.

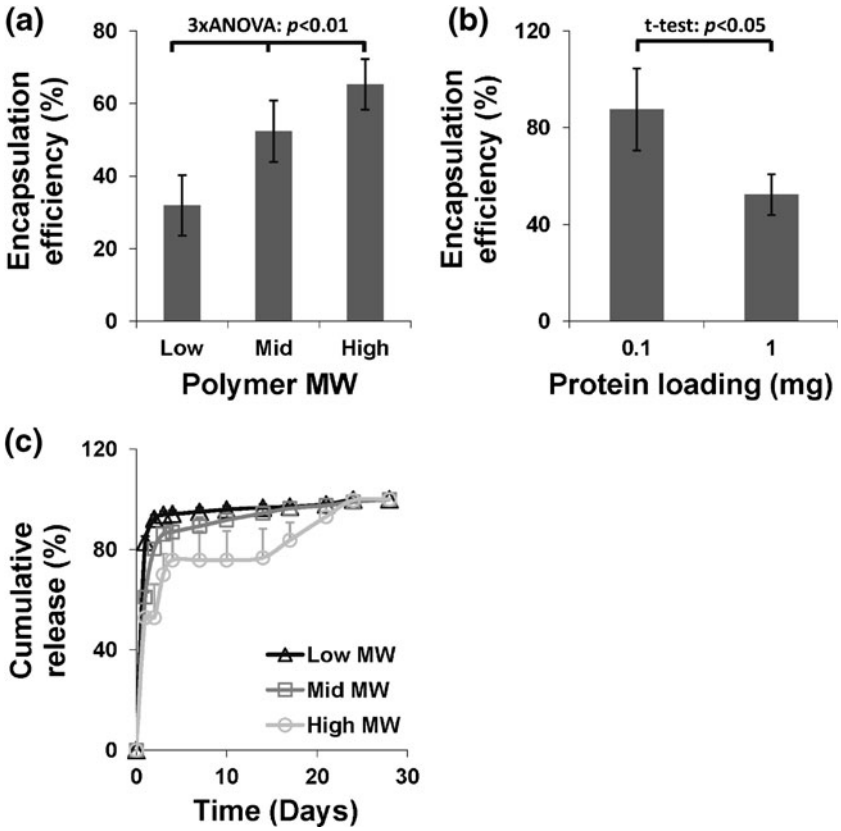

Fig. 2 Encapsulation efficiency and release kinetics of ribonuclease-I from PLGA particles. Encapsulation efficiency of ribonuclease-I in particles with different PLGA molecular weights (low: 0.26–0.54 dL/g, mid: 0.55–0.75 dL/g, high: 0.95–1.20 dL/g) (**a**) and initial protein loadings (**b**). Cumulative release of ribonuclease-I from particles made with different PLGA molecular weights (low: 0.26–0.54 dL/g, mid: 0.55–0.75 dL/g, high: 0.95–1.20 dL/g) (**c**) (n=3)

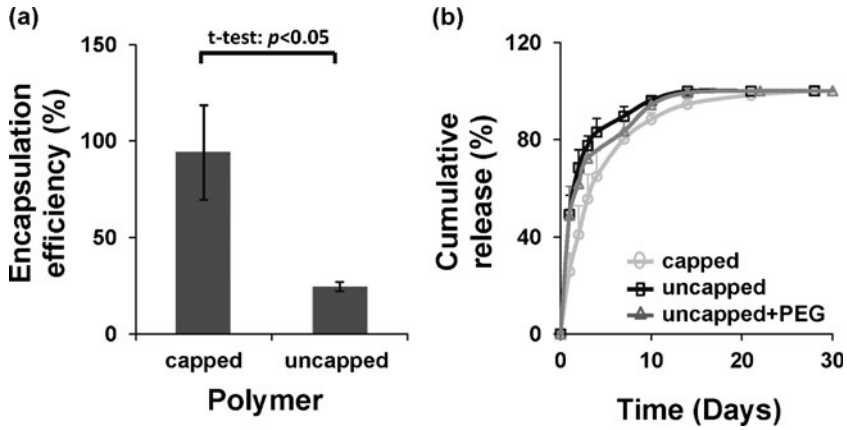

Fig. 3 Encapsulation efficiency and release kinetics of BMP2 from PLGA particles. BMP2 encapsulation efficiency in capped and uncapped PLGA particles (**a**). Cumulative release of BMP2 from capped PLGA, capped PLGA with the addition of PEG400, or uncapped PLGA (**b**). Preparations were made with PLGA of 0.55–0.75 dL/g molecular weight of and a lactide-to-glycolide ratio of 50:50 (n=3)

3.5 hMSCs osteogenic differentiation on ZrO_2 scaffolds

hMSCs were cultivated on ZrO_2 scaffolds for 60 days in an undifferentiating growth medium or in an osteoinductive medium. As seen by confocal microscopy, the undifferentiated cells (Fig. 5a) grew extensively and filled the scaffold's pores, while in the same period of time osteogenic-induced cells only grew on the pores' surface (Fig. 5b). Von Kossa staining performed on scaffold-seeded cells revealed high mineralization of the scaffold cultivated with osteogenic-induced hMSCs (Fig. 5d, indicated by brown coloring) in comparison to scaffolds cultivated with undifferentiated hMSCs (Fig. 5c).

3.6 Co-culturing hMSCs and HUVECs on ZrO_2 scaffolds

Cultured hMSCs proliferated rapidly on ZrO_2 scaffolds for the first 3 weeks, reaching steady-state growth around $3.5\ 10^5$ cells per scaffold (Fig. 6a). In contrast, HUVECs alone did not survive on ZrO_2 scaffolds (Fig. 6b). However, hMSCs seeding and culturing on ZrO_2 scaffolds 2 weeks prior to the seeding of HUVECs expressing GFP enabled the growth and proliferation of HUVECs-GFP over a period of a month (Fig. 6c).

3.7 Production of a composite ZrO_2 scaffold and hMSCs cultivation

Scanning electron microscopy was used to study the surfaces of ZrO_2 scaffolds and composite scaffolds (Fig. 7a and b). Carbodiimide chemistry was used to create the composite scaffold in which PLGA microspheres are seen (Fig. 7b). Cell growth of hMSCs cultivated on the composite scaffolds had a slower initial growth rate compared to hMSCs grown on 'clean' scaffolds; however, after 3 weeks cell density was similar, fluctuating around $3.0 \cdot 10^5$ cells per scaffold (Fig. 7c).

4 Discussion

Bone tissue engineering is an alternative approach for the treatment of delayed union or non-union fractures. Engineering a three-dimensional substitute for bone tissue regeneration is a multi-step process that needs to take into consideration cell and scaffold parameters. For a tissue to be fully constructed, one also needs vascularization and growth factors such as BMP2 that will enhance proper bone formation. In this study we demonstrate the use of PLGA microspheres as a BMP2 delivery system that can be incorporated into ZrO_2 scaffolds used for bone regeneration.

In our experiments we succeeded in producing spherical, non-porous and micro-sized PLGA particles that can be loaded with the desired protein. The size, encapsulation efficiency, and release kinetics of the delivery system have an important effect on the total dose and duration of protein release. These parameters are affected by the protein's partition coefficient, the polymer's molecular weight, and the initial loading of the protein. To optimize these parameters, we used capped PLGA polymers (ester end-group) and ribonuclease-I as a model protein, given that it has a similar isoelectric point and molecular weight as our target protein, BMP2, and it is more affordable. Using a higher molecular weight PLGA polymer resulted in particles with increased size, increased encapsulation efficiency, and reduced burst release, which is in line with previous work (Hamishehkar et al. 2009; Viswanathan et al. 1999). The higher molecular weight PLGA probably created a more viscous primary emulsion, which can better sustain the homogenization forces, hence yielding larger microspheres (Mehta et al. 1996; Mohamed and van der Walle 2008). Additionally, lower molecular weight polymers are more soluble in the organic phase, leading to longer solidification time, resulting in increased diffusion of the protein in the non-solidified matrix. The increased diffusion facilitates the extraction of the protein to the surface of the microspheres and into the continuous aqueous phase (Mehta et al. 1996; Yeo and Park

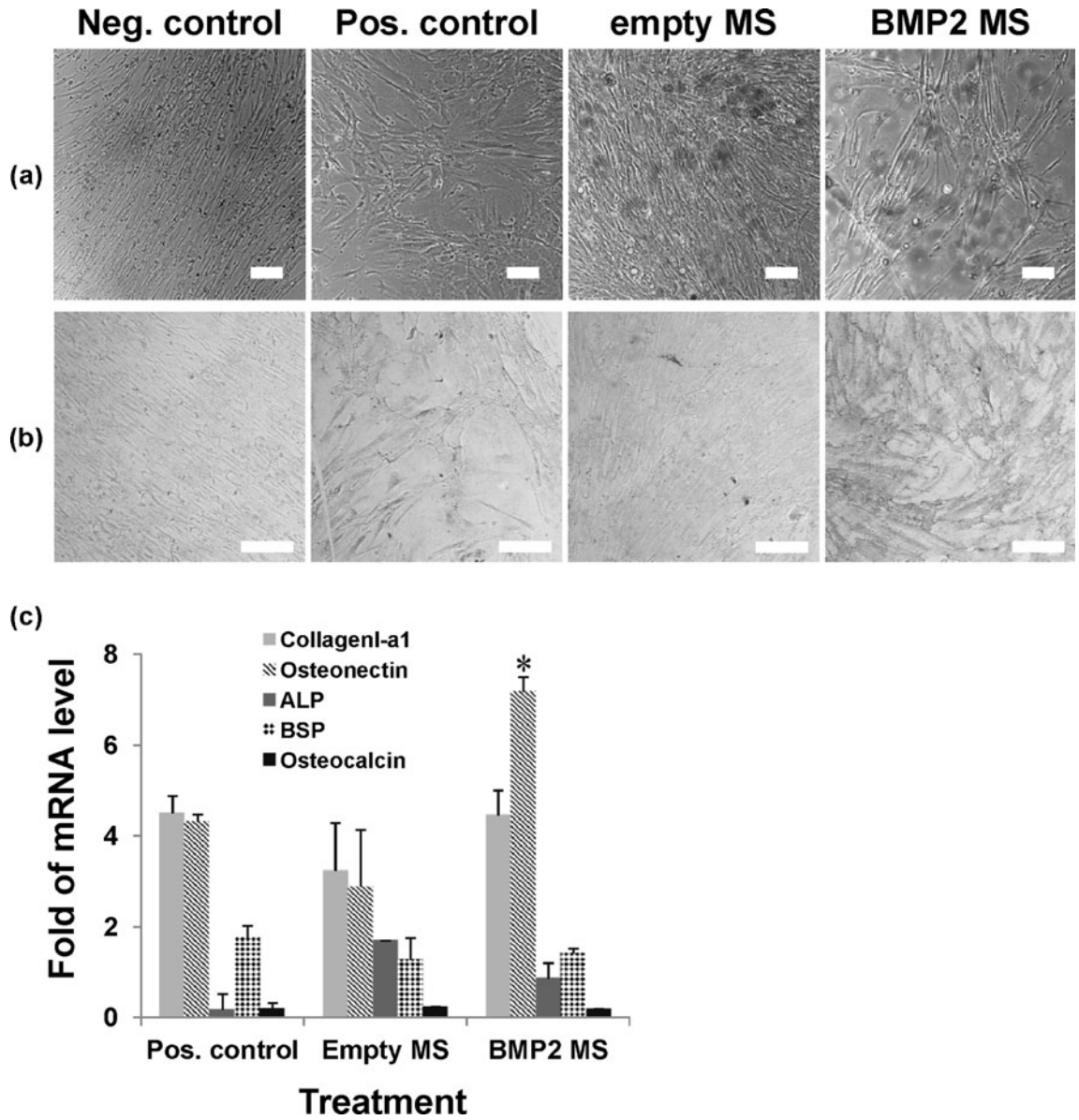

Fig. 4 Biological effect of BMP2 released from PLGA particles on cell morphology (**a**) and calcium deposition (**b**) on hMSCs. Light microscopy images of hMSCs cultivated for 12 days with growth medium (negative control), growth medium supplemented with 100 ng/ml BMP2 (positive control), growth medium with empty microspheres (Empty MS), and growth medium with BMP2 loaded microspheres (BMP2 MS). mRNA expression levels of collagen-I, osteonectin, alkaline phosphatase (ALP), bonesialoprotein (BSP) and osteocalcin in MSCs (**c**). The results are calculated as the mRNA level for each treatment group normalized to GAPDH, divided by the mRNA level of undifferentiated hMSCs (negative control) (n=3)

2004). The lower molecular weight preparations also had a smaller particle size, resulting in a higher ratio of surface area to volume, thus increasing the protein diffusion (Allison 2008; Yeo and Park 2004). The last parameter affecting the encapsulation efficiency, which we tested, is the initial protein concentration used for loading the PLGA particles. Our results show that when the protein concentration was increased, the loading efficiency decreased dramatically. It may be that for each protein, there is a maximal amount of protein that could be entrapped in the PLGA microspheres depending on the protein partition coefficient and size.

After optimizing the microencapsulation process with a model protein, BMP2 encapsulation efficiency and its release kinetics were studied. In this set of experiments particles prepared with capped (ester end-group) and uncapped (carboxylic end-group) PLGA polymers were studied. These two types of polymers were investigated because one of our approaches to incorporating the microspheres into the ZrO_2 scaffolds is based on carbodiimide chemistry, which involves the reaction of a carboxylic group. Using capped PLGA led to high encapsulation efficiency (94 %), similar to previously reported studies (Isobe et al. 1996; Kempen

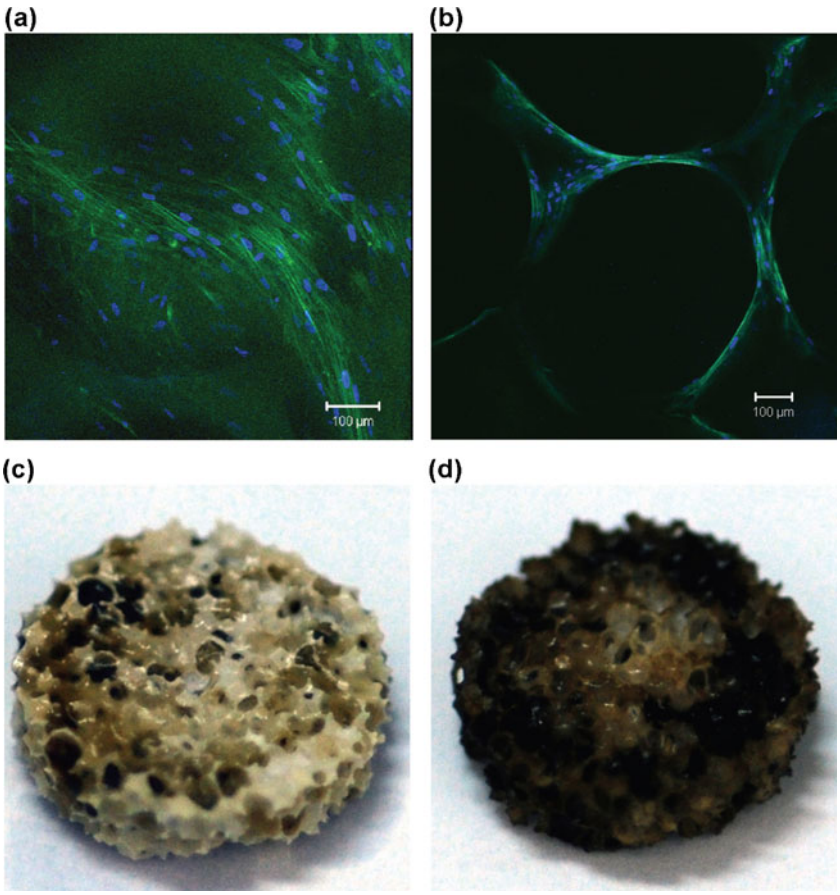

Fig. 5 Osteogenic differentiation of hMSCs on ZrO_2 scaffolds. Fluorescent micrographs of hMSCs (**a**) and osteogenic induced hMSCs (**b**). Cell nuclei marked with DAPI (*blue*) and actin fibers are marked with phalloidin-FITC (*green*). Von Kossa staining of **c** hMSCs and **d** osteogenesic induced hMSCs after 60 days of cultivation on ZrO_2. *Brown* color indicates calcium deposition

et al. 2008; Kempen et al. 2009; Lochmann et al. 2010; Ruhe et al. 2003). On the other hand, the use of the uncapped polymer resulted in reduced encapsulation efficiency (24.6 %) and a higher burst release (49 %) compared to the capped polymer preparations (26 %). This finding could indicate that hydrophobic interactions are the dominate forces between the BMP2 and the polymer, as polymers with ester end groups are capable of more hydrophobic interactions, also leading to slower water penetration, resulting in slower diffusion of the protein. In contrast to our results, Ruhe et al. and Li et al. demonstrated a burst release of less than 5 % using similar polymer composition (Li et al. 2009; Ruhe et al. 2003). In the latter studies, however, a carrier protein was used and only 18 % of the encapsulated protein was released over 4 weeks. Aiming to decrease the burst release, we added PEG to the internal phase during preparation of the primary emulsion, in order to limit protein penetration to the interfacial film of the primary water-in-oil emulsion, thus decreasing protein anchorage to the polymer layer (Dorati et al. 2005; Pean et al. 1999). Unfortunately, the addition of PEG400 to the preparation with an uncapped PLGA polymer did not lead to a decrease in the burst release. These results are in line with Kang et al. who also added PEG to the microsphere preparation and demonstrated an increase in the burst release that was attributed to the porous morphology of the microspheres produced with PEG (Kang and Singh 2001).

The PLGA microsphere preparation procedure involves the use of organic solvents and mechanical forces, which may affect the activity of the encapsulated protein. Therefore, we studied the biological activity of the released BMP2 from the microspheres. Our results clearly demonstrate that BMP2 retained its biological activity and hMSCs cultivated with BMP2-loaded microspheres showed a distinct morphology and grew in clusters similarly to hMSCs cultivated with free BMP2. These results are supported by Rodrıguez et al. who reported that osteogenic differentiation of hMSCs was accompanied by considerable alterations in morphological and cytoskeletal organization when cultured in an osteo-differentiation medium (Rodriguez et al. 2004). After 2 weeks of cultivation with the BMP2-loaded PLGA microspheres, the hMSCs showed increased expression levels of the collagen-I and osteonectin genes—indicative of osteogenic differentiation. Nevertheless, other osteogenes such as osteocalcin, alkaline phosphatase and bonesialoprotein were not induced by free BMP2 or BMP2 released from PLGA microspheres. It is possible that the cultivation time was not sufficient to induce changes in the expression levels of these

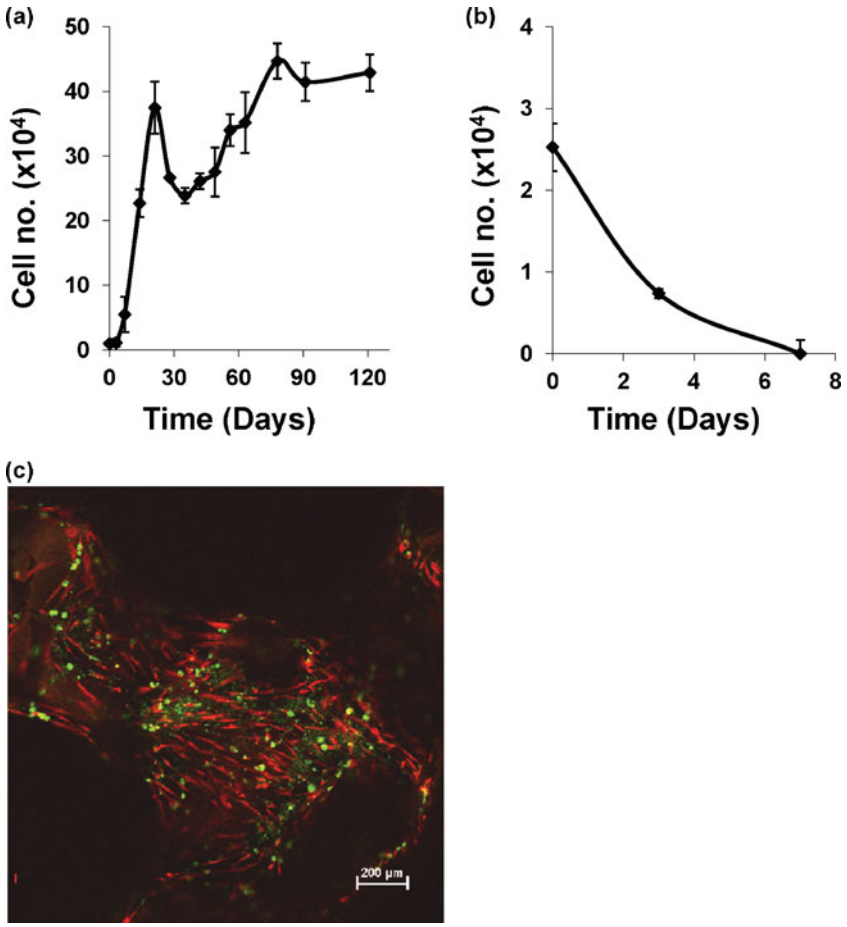

Fig. 6 Cell cultivation on ZrO_2 scaffolds. Viability of hMSCs (**a**) and HUVECs (**b**) cultured on a ZrO_2 scaffold (n=3). Confocal micrographs of hMSCs and HUVECs-GFP (*green*) cultivated on a ZrO_2 scaffold for 30 days (**c**). Cells were fixed and stained with propidium iodide (*red*)

genes or that the expression of different genes is elevated during the first days of cultivation and then decreases to control levels. This hypothesis is supported by previous studies demonstrating that the expression levels of these genes, aside from the collagen-I gene, are time dependent (Frank et al. 2002; Jaiswal et al. 1997; Shea et al. 2003; Suck et al. 2007). A study by Shea et al. showed that addition of BMP2 resulted in high levels of collagen-I throughout the entire cultivation period, while the level of osteocalcin was elevated on day 10, and the level of osteocalcin was elevated on day 2 and 16 (Shea et al. 2003). Studies also showed that alkaline phosphatase levels increased in the first days and then decreased to control levels (Frank et al. 2002; Jaiswal et al. 1997; Suck et al. 2007). Finally, we addressed the growth of cells on the ceramic ZrO_2 scaffold and the release of BMP2 from the PLGA particles added to the scaffold. The ceramic ZrO_2 scaffolds possess a macroporous structure connected via micro porous channels, resulting in a large surface area enabling cell adherence, growth and extracellular matrix production. In our studies, osteogenic-induced hMSCs showed high mineralization of the scaffold by deposition of calcium, although their growth rate was slower in comparison to the undifferentiated hMSCs, which grew extensively and filled the scaffold's pores. In contrast, the ZrO_2 scaffold did not support HUVEC growth and proliferation. This observation may consistent with the fact that HUVECs need an appropriate matrix in order to adhere and proliferate (Deb et al. 2010; Thimm et al. 2008). In addition, many biomaterials are pre-coated with fibronectin, laminin, gelatin or collagen, which enhance HUVEC viability (Deb et al. 2010; Thimm et al. 2008). As we did not want to alter the ZrO_2 scaffold or composition, we addressed this problem of enhancing HUVEC viability and proliferation by pre-culturing the scaffolds with hMSCs. The rationale behind this was that the hMSCs cultured on the ZrO_2 scaffolds would secrete an extracellular matrix that may support the adherence and proliferation of HUVECs. In addition, it is well known that osteoblastic and osteoprogenitor cells secrete VEGF (vascular endothelial growth factor), which is a potent angiogenic growth factor that stimulates endothelial cell proliferation (Rouwkema et al. 2006; Rouwkema et al. 2008; Santos and Reis 2010). Co-culturing endothelial cells with osteoblast cells is also known to stimulate vessel-like structure formation, which were not formed in mono-cultures of HUVECs, and that these co-cultures are superior in effective bone formation *in vivo* (Hofmann et al. 2008; Kim et al. 2008). Our co-culture experiments on the ZrO_2 scaffolds demonstrated that hMSCs succeeded in developing a surrounding, which enhanced adherence and proliferation of

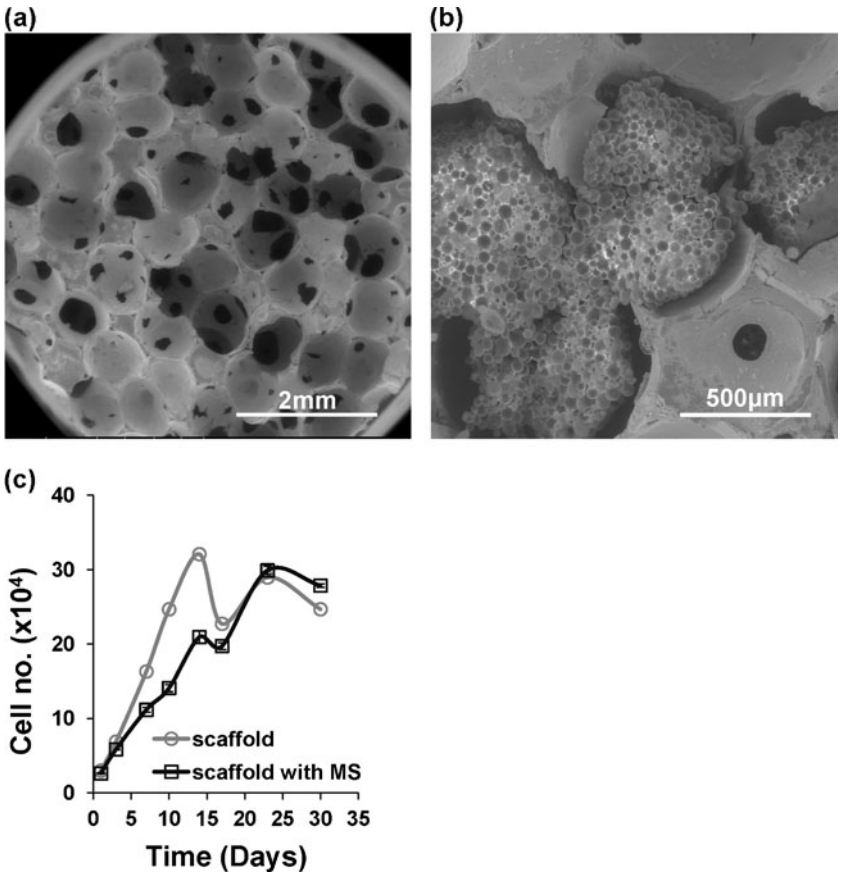

Fig. 7 ZrO_2 and composite scaffolds and hMSCs cultivation. Scanning electron microscopy images of a ZrO_2 scaffold (**a**) and a composite ZrO_2 scaffold incorporated with PLGA particles (**b**). Viability of hMSCs seeded on ZrO_2 scaffolds and composite scaffolds over time (**c**) (n=3)

HUVECs. Nonetheless, more studies focusing on the osteogenic differentiation potential of hMSCs, and vessel formation by endothelial cells in the co-culture need to be pursued.

Finally, we addressed the importance of supplementing the scaffold with appropriate growth factors, which can enhance bone formation. Most polymer-ceramic composites studied to date are based on ceramic particles that are added to a polymeric scaffold or are laid on calcium phosphate cements embedded with PLGA particles (Habraken et al. 2007). Polymeric scaffolds with added ceramic particles lack mechanical properties, while calcium phosphate cements embedded with PLGA particles show incomplete release of the encapsulated therapeutics. In our work we aimed to develop a composite scaffold, comprising a ZrO_2 component and a polymeric delivery component that can deliver the required factors. Therefore, our approach was to incorporate PLGA microspheres into the porous structure of ZrO_2 scaffolds using carbodiimide chemistry. Scanning electron microscopy studies have shown that a large amount of microspheres was introduced into the ZrO_2 scaffold. However, the microspheres' morphology appeared to be altered by the chemical reaction and the microspheres formed aggregates. It is possible that the polymer's carboxylic end groups reacted with each other to create acid anhydrides. Another possibility is that the polymer's carboxylic end groups could have reacted with amine groups of proteins located on the surface of the microspheres. Nevertheless, the ZrO_2 scaffolds and bone marrow-derived hMSCs demonstrate that the composite scaffolds support cell growth and that the favored surface properties of the scaffold, in respect to cell adhesion and proliferation, were not affected by the modification of the scaffold with PLGA microparticles. Moreover, hMSCs demonstrated a rapid growth rate for the first 3 weeks, at which time it plateaued. These findings are in contrast to Suck and Roeker et al., who observed a decrease phase in the number of preosteoblastic cells after 2 weeks of cultivation on ZrO_2 scaffolds (Roeker et al. 2009; Suck et al. 2007). Our results also differ from Seebach et al., who cultured hMSCs on six different scaffolds for bone regeneration, and showed that the number of hMSCs that adhered remained constant over the 10 days (Seebach et al. 2010).

5 Conclusions

We have succeeded in developing a composite system that is based on PLGA microspheres entrapping BMP2, integrated into a ZrO_2 scaffold. We have demonstrated that although using harsh conditions for the preparation of PLGA particles, the BMP2 released from PLGA microspheres retained its

biological activity and osteoblastic marker expression was induced in hMSCs. The composite scaffold has the mechanical properties of the ZrO_2 scaffold and the PLGA particles exhibit a full release of the growth factor, given that they are not fully embedded within the ceramic component. Nonetheless, further investigation of the osteogenic differentiation of hMSCs cultivated on the composite scaffolds is warranted. We successfully co-cultured hMSCs with endothelial cells that could enable construction of a pre-vascular network that will overcome limitations of nutrient and oxygen diffusion into the scaffold. Positive results from future studies will further confirm the potential of such composite scaffolds for bone tissue regeneration.

Acknowledgments The research was supported by the Niedersachsen Foundation. The partial support of the Russell Berrie Nanotechnology Institute, Technion–Israel Institute of Technology (IIT), is thankfully acknowledged. bFGF was kindly donated by Prof. Gera Neufeld, from the Department of Anatomy and Cell Biology, Faculty of Medicine, IIT. BMP2 was kindly donated by Prof. Walter Sebald, from Biozentrum University, Würzburg, Germany. We further wish to thank Ilana Schoenbrun for her technical assistance.

References

S.D. Allison, J. Pharm. Sci. **97**, 2022–2035 (2008)
F. Barry, R.E. Boynton, B. Liu, J.M. Murphy, Exp Cell Res. **268**, 189–200 (2001)
O. Benny, M. Duvshani-Eshet, T. Cargioli, L. Bello, A. Bikfalvi, R.S. Carroll, M. Machluf, Clin. Cancer Res. **11**, 768–776 (2005)
C. Berkland, K. Kim, D.W. Pack, Pharm. Res. **20**, 1055–1062 (2003)
C. Berkland, M. King, A. Cox, K. Kim, D.W. Pack, J Control Release. **82**, 137–147 (2002)
M. Braddock, P. Houston, C. Campbell, P. Ashcroft, News Physiol Sci. **16**, 208–213 (2001)
A.I. Caplan, J. Cell. Physiol. **213**, 341–347 (2007)
R.R. Chen, E.A. Silva, W.W. Yuen, D.J. Mooney, Pharm. Res. **24**, 258–264 (2007)
C. Colnot, Tissue Eng Part B Rev. **17**, 449–457 (2011)
N. Dahan, G. Zarbiv, U. Sarig, T. Karram, A. Hoffman, M. Machluf, Tissue Eng Part A. **18**, 411–422 (2012)
S. Deb, R. Mandegaran, L. Di Silvio, J Mater Sci Mater Med. **21**, 893–905 (2010)
M. Dominici, K. Le Blanc, I. Mueller, I. Slaper-Cortenbach, F. Marini, D. Krause, R. Deans, A. Keating, D. Prockop, E. Horwitz, Cytotherapy **8**, 315–317 (2006)
R. Dorati, I. Genta, L. Montanari, F. Cilurzo, A. Buttafava, A. Faucitano, B. Conti, J Control Release. **107**, 78–90 (2005)
O. Frank, M. Heim, M. Jakob, A. Barbero, D. Schafer, I. Bendik, W. Dick, M. Heberer, I. Martin, J. Cell. Biochem. **85**, 737–746 (2002)
M. Grellier, L. Bordenave, J. Amedee, Trends Biotechnol. **27**, 562–571 (2009)
E.H. Groeneveld, E.H. Burger, Eur. J. Endocrinol. **142**, 9–21 (2000)
W.J. Habraken, J.G. Wolke, J.A. Jansen, Adv Drug Deliv Rev. **59**, 234–248 (2007)
Z.S. Haidar, R.C. Hamdy, M. Tabrizian, Biotechnol. Lett. **31**, 1817–1824 (2009)
H. Hamishehkar, J. Emami, A.R. Najafabadi, K. Gilani, M. Minaiyan, H. Mahdavi, A. Nokhodchi, Colloids Surf B Biointerfaces. **74**, 340–349 (2009)
A. Hofmann, U. Ritz, S. Verrier, D. Eglin, M. Alini, S. Fuchs, C.J. Kirkpatrick, P.M. Rommens, Biomaterials **29**, 4217–4226 (2008)
M. Isobe, Y. Yamazaki, S. Oida, K. Ishihara, N. Nakabayashi, T. Amagasa, J. Biomed. Mater. Res. **32**, 433–438 (1996)
R.A. Jain, Biomaterials **21**, 2475–2490 (2000)
N. Jaiswal, S.E. Haynesworth, A.I. Caplan, S.P. Bruder, J. Cell. Biochem. **64**, 295–312 (1997)
P. Johansen, Y. Men, R. Audran, G. Corradin, H.P. Merkle, B. Gander, Pharm. Res. **15**, 1103–1110 (1998)
T. Joki, M. Machluf, A. Atala, J. Zhu, N.T. Seyfried, I.F. Dunn, T. Abe, R.S. Carroll, P.M. Black, Nat. Biotechnol. **19**, 35–39 (2001)
F. Kang, J. Singh, AAPS PharmSciTech **2**, 30 (2001)
J.M. Karp, G.S. Leng Teo, Cell stem cell **4**, 206–216 (2009)
T. Kaully, K. Kaufman-Francis, A. Lesman, S. Levenberg, Tissue Eng Part B Rev. **15**, 159–169 (2009)
D.H. Kempen, L. Lu, T.E. Hefferan, L.B. Creemers, A. Maran, K.L. Classic, W.J. Dhert, M.J. Yaszemski, Biomaterials **29**, 3245–3252 (2008)
D.H. Kempen, M.J. Yaszemski, A. Heijink, T.E. Hefferan, L.B. Creemers, J. Britson, A. Maran, K.L. Classic, W.J. Dhert, L. Lu, J Control Release. **134**, 169–176 (2009)
Y. Khan, M.J. Yaszemski, A.G. Mikos, C.T. Laurencin, J Bone Joint Surg Am. **90**(Suppl 1), 36–42 (2008)
J.S. Kim, J.H. Chang, H.K. Yu, J.H. Ahn, J.S. Yum, S.K. Lee, K.H. Jung, D.H. Park, Y. Yoon, S.M. Byun et al., J. Biol. Chem. **278**, 29000–29008 (2003)
S. Kim, S.S. Kim, S.H. Lee, S. Eun Ahn, S.J. Gwak, J.H. Song, B.S. Kim, H.M. Chung, Biomaterials **29**, 1043–1053 (2008)
B. Li, T. Yoshii, A.E. Hafeman, J.S. Nyman, J.C. Wenke, S.A. Guelcher, Biomaterials **30**, 6768–6779 (2009)
J.R. Lieberman, A. Daluiski, T.A. Einhorn, J Bone Joint Surg Am. **84-A**, 1032–1044 (2002)
A. Lochmann, H. Nitzsche, S. von Einem, E. Schwarz, K. Mader, J Control Release. **147**, 92–100 (2010)
M. Lovett, K. Lee, A. Edwards, D.L. Kaplan, Tissue Eng Part B Rev. **15**, 353–370 (2009)
J.M. Lu, X. Wang, C. Marin-Muller, H. Wang, P.H. Lin, Q. Yao, C. Chen, Expert Rev Mol Diag. **9**, 325–341 (2009)
R.C. Mehta, B.C. Thanoo, P.P. DeLuca, J Control Release. **41**, 249–257 (1996)
F. Mohamed, C.F. van der Walle, J. Pharm. Sci. **97**, 71–87 (2008)
V. Mourino, A.R. Boccaccini, J R Soc Interface. **7**, 209–227 (2010)
J. Mullerad, S. Cohen, E. Voronov, R.N. Apte, Cytokine **12**, 1683–1690 (2000)
J.M. Pean, F. Boury, M.C. Venier-Julienne, P. Menei, J.E. Proust, J.P. Benoit, Pharm. Res. **16**, 1294–1299 (1999)
J.R. Porter, T.T. Ruckh, K.C. Popat, Biotechnol. Prog. **25**, 1539–1560 (2009)
A.H. Reddi, Nat. Biotechnol. **16**, 247–252 (1998)
T.P. Richardson, M.C. Peters, A.B. Ennett, D.J. Mooney, Nat. Biotechnol. **19**, 1029–1034 (2001)
J.P. Rodriguez, M. Gonzalez, S. Rios, V. Cambiazo, J. Cell. Biochem. **93**, 721–731 (2004)
S. Roeker, S. Bohm, S. Diederichs, F. Bode, A. Quade, V. Korzhikov, M. van Griensven, T.B. Tennikova, C. Kasper, J Biomed Mater Res B Appl Biomater **91**, 153–162 (2009)
C. Rosada, J. Justesen, D. Melsvik, P. Ebbesen, M. Kassem, Calcif. Tissue Int. **72**, 135–142 (2003)
J. Rouwkema, J. de Boer, C.A. Van Blitterswijk, Tissue Eng. **12**, 2685–2693 (2006)
J. Rouwkema, N.C. Rivron, C.A. van Blitterswijk, Trends Biotechnol. **26**, 434–441 (2008)

P.Q. Ruhe, E.L. Hedberg, N.T. Padron, P.H. Spauwen, J.A. Jansen, A.G. Mikos, J Bone Joint Surg Am. **85-A**(Suppl 3), 75–81 (2003)
A.J. Salgado, O.P. Coutinho, R.L. Reis, Macromol. Biosci. **4**, 743–765 (2004)
M.I. Santos, R.L. Reis, Macromol. Biosci. **10**, 12–27 (2010)
C. Seebach, J. Schultheiss, K. Wilhelm, J. Frank, D. Henrich, Injury **41**, 731–738 (2010)
C.M. Shea, C.M. Edgar, T.A. Einhorn, L.C. Gerstenfeld, J. Cell. Biochem. **90**, 1112–1127 (2003)
K. Suck, L. Behr, M. Fischer, H. Hoffmeister, M. van Griensven, F. Stahl, T. Scheper, C. Kasper, J Biomed Mater Res A. **80**, 268–275 (2007)
B.W. Thimm, R.E. Unger, H.G. Neumann, C.J. Kirkpatrick, Biomed. Mater. **3**, 015007 (2008)
J.K. Vasir, V. Labhasetwar, Adv Drug Deliv Rev. **59**, 718–728 (2007)
N.B. Viswanathan, P.A. Thomas, J.K. Pandit, M.G. Kulkarni, R.A. Mashelkar, J Control Release. **58**, 9–20 (1999)
E. Walter, D. Dreher, M. Kok, L. Thiele, S.G. Kiama, P. Gehr, H.P. Merkle, J Control Release. **76**, 149–168 (2001)
E. Walter, K. Moelling, J. Pavlovic, H.P. Merkle, J Control Release. **61**, 361–374 (1999)
Y.T. Xiao, L.X. Xiang, J.Z. Shao, Biochem. Biophys. Res. Commun. **362**, 550–553 (2007)
Y. Yeo, K.N. Park, Arch Pharm Res. **27**, 1–12 (2004)